Effect of the classical electron Coulomb crystal on interedge magnetoplasmons

A. M. C. Valkering, P. K. H. Sommerfeld,* and R. W. van der Heijden
Department of Physics, Eindhoven University of Technology, P.O. Box 513, NL 5600 MB Eindhoven, The Netherlands
(Received 26 January 1998)

Measurements of the linewidths of interedge magnetoplasmons are reported for electrons on liquid helium in a temperature range from 200 to 600 mK and in a magnetic field $B=1$ T. The linewidths show an abrupt increase at a certain temperature. This temperature changes if the electron density is altered and can be related to the crystallization temperature. At the frequencies used, the effect on conventional edge magnetoplasmons is only very weak. [S0163-1829(98)05828-7]

I. INTRODUCTION

As was first pointed out by Crandall and Williams[1] it is possible for a classical two-dimensional (2D) system to crystallize. This crystallization is often referred to as Wigner crystallization, despite the fact that Wigner studied crystallization in a three-dimensional quantum gas.[2] Although the Coulomb crystal has been observed in many different systems, such as, e.g., trapped atomic ions,[3] dusty rf plasmas,[4] colloidal suspensions,[5] and ions below the surface of liquid helium,[6] classical 2D Coulomb crystals from the 2D electron system on liquid helium[7] are the most extensively investigated. It is a simple and pure system where the only impurities on the surface are ^{3}He atoms.[8] Another advantage is the possibility of varying the screening, going from an unscreened system (bulk helium) to a screened system (helium films).[9,10]

So far, a number of methods have been used to observe and investigate the properties of the crystal: plasma resonances of the crystal (coupled to the capillary waves on the He surface),[7,11] measurements of the shear in the crystal,[12,13] mobility measurements,[14] and recently, measurements of the magnetoconductivity.[15–17] The measurements of the magnetoconductivity have shown that although the conductivity is different from the conductivity in the fluid, the crystal is still an excellent conductor.

In the fluid phase edge magnetoplasmons (EMP's) have been studied extensively both in the low- (Refs. 18 and 19) and the high-field limit.[20] EMP's are charge-density fluctuations that propagate along the edge due to the Hall effect. For high magnetic fields they are localized near the boundary of the electron sheet. Since the current flows nearly perpendicular to the electric field, the damping of the EMP, which is proportional to the parallel magnetoconductivity σ_{xx},[21] is low. Therefore they can be observed even at low frequencies ω, when $\omega\tau \ll 1$ (τ is the scattering rate of the electrons). The propagation velocity v of the EMP is the Hall velocity E/B (E is the electric field due to the charge perturbations, B is the magnetic field), which in turn is proportional to the Hall conductivity σ_{xy}.[21] The inverse proportionality of the EMP frequency to the magnetic field is one of the most characteristic properties of EMP's.

A more general form of the EMP is the interedge magnetoplasmon (IEMP), located at the *boundary* between two 2DES's with different electron densities.[22,23] The IEMP frequency is proportional to the *difference* of the Hall conductivities at either side of the boundary. The damping is determined by the *average* σ_{xx}.

EMP's have proved to be very useful to study transport in a 2DES in addition to the commonly used Corbino geometry,[24] since their damping is proportional to σ_{xx}. An alternative method for investigating transport in the crystal is of interest, in view of the issue of compatibility of Corbino geometry and rigid rotation of the crystal.[16] However, in the convenient low-frequency domain, i.e., $\omega \ll \omega_p$, the plasma frequency, the EMP properties seem not to change at the melting transition.[18,23,24] A complication here is that the EMP is located in the region of vanishing density.[20] In low magnetic fields, where the EMP frequency is in the order of the plasma frequency, the properties of the EMP resemble the zero-field plasmon properties. In particular, its frequency depends on the effective mass. Therefore, at the melting transition frequency shifts are expected and have been observed.[25] This regime has so far not been used for σ_{xx} determination.

The purpose of the present work is to investigate the effect of crystallization on the low-frequency IEMP's, located at a boundary between two 2DES's with different electron density. The differences of IEMP's, relevant for the sensitivity to crystallization, as compared to EMP's are twofold: (1) the shape of the density step is different and most importantly (2) everywhere on the step the 2DES is in or near the crystal phase.

We present measurements of linewidths of IEMP's for varying electron densities at one side of the boundary. The linewidths show an abrupt increase below a certain temperature that can be related to the melting transition. Additional measurements to confirm this are also shown: It will be shown that the linewidth increase is a function of the *absolute* electron density and that the dependence of the linewidth on the drive voltage is different below and above crystallization. Preliminary measurements were published in Ref. 26.

II. EXPERIMENTAL TECHNIQUES

The experimental cell consists of two circular metal plates (top plate and bottom plate) with a cylindrical electrode (guard ring) in between [see Fig. 1(a)]. The cell is 3 mm high and has an inner diameter of 15 mm. It was filled with liquid helium to a level of 1 mm above the bottom plate, which was

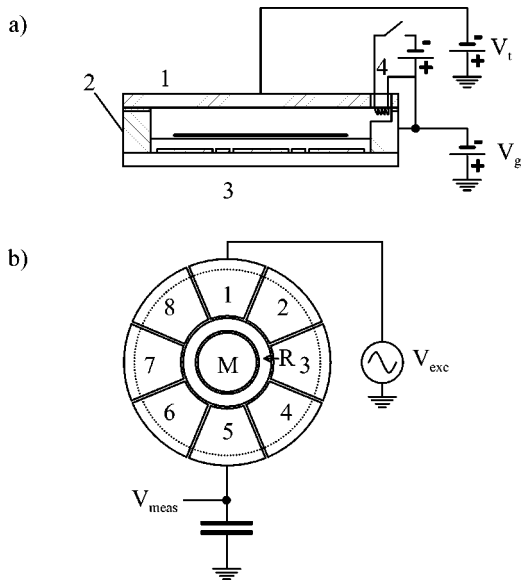

FIG. 1. (a) Experimental cell with 1, top plate; 2, guard ring; 3, bottom plate with electrodes; and 4, filament. (b) Electrode structure on bottom plate; M, middle electrode; R, ring electrode; and 1–8, outer electrode segments.

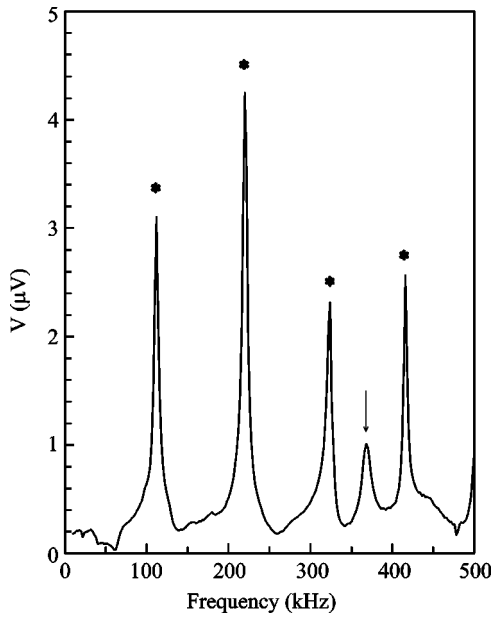

FIG. 2. Frequency spectrum from 10 to 500 kHz. EMP resonances are marked with an asterisk, the IEMP resonance is indicated by an arrow. The temperature $T=563$ mK, inner density $n_1=2.3\times10^{12}$ m^{-2}, outer density $n_2=0.58\times10^{12}$ m^{-2}.

checked by measuring the capacitance from the top to the bottom plate. The bottom plate is divided into ten electrodes [see Fig. 1(b)]: a circular middle electrode with a ring electrode surrounding it and an outer ring electrode divided into eight segments. Both the top plate and the guard ring are at a negative dc voltage (V_t and V_g, respectively) to provide the holding field and confinement. In the measurements V_t was typically -10 V. The ratio V_g/V_t was 3/2 in all measurements.

The surface was charged to saturation with electrons using a filament that was located in a small hole in the guard ring. By applying a positive (or negative) voltage to the middle and ring electrode an electron sheet with a higher (or lower) density in the center was obtained as in Ref. 23. Typical values for the electron densities are between 0 and 2.3 $\times10^{12}$ m^{-2} for the inner electron density n_1 and 0.58 $\times10^{12}$ m^{-2} for the outer electron density n_2. To be sure that saturation was reached the surface was first charged with high voltages on the electrodes (-100 V and -67 V on the guard and the top plate, $+50$ V on the middle and the ring electrode) and afterwards decreased to the voltages that were used during the measurements.

To measure the response of the 2DES an ac voltage of 10 mV in a frequency range from 10 to 500 kHz was applied to one of the eight outer electrodes and the induced voltage at the opposite electrode was measured with a coaxial cable lead using a lock-in amplifier. Since the impedance due to the capacitance of the lead coaxial cable is much smaller than the impedance between excitation and detection electrode, the method effectively corresponds to measuring current to ground. The frequency range used is too high for using a sensitive current preamplifier. All measurements were done in a magnetic field B of 1 T normal to the surface.

III. RESULTS

A. IEMP linewidths as a function of temperature

To study the linewidths of IEMP, first a frequency spectrum was measured from 10 to 500 kHz, as shown in Fig. 2, to identify both the EMP's and IEMP's. For the EMP four harmonics are visible, marked with an asterisk. The IEMP is visible at 360 kHz with a smaller amplitude and a somewhat larger linewidth. In general, the dispersion relation $\omega(k)$ for the (I)EMP's is given by[22,23]

$$\omega=\frac{\alpha|n_1-n_2|e}{\varepsilon_0\varepsilon_r B}k, \tag{1}$$

where e is the elementary charge, $\varepsilon_0\varepsilon_r$ the permittivity, k the wave vector, and $|n_1-n_2|$ the difference in electron density across the boundary (for EMP's n_2 is 0). α is a parameter of the order of 1 that depends on the density profile at the boundary. Its value is higher when the density profile is steeper. Theoretically α depends logarithmically on σ_{xx} and k, but this dependence is ignored here. Due to different circumferences [see Fig. 1(b)] the wave vector at resonance is a factor of 2 higher for the IEMP than for the EMP. For the data in Fig. 2 $|n_1-n_2|$ is a factor of 3 higher than n_2. The resonance position of the IEMP would thus be expected at a six times higher frequency than the EMP (i.e., 600 kHz). The observed resonance occurs at 360 kHz. The shift is attributed to different α's in case of IEMP and EMP in agreement with earlier measurements[23] ($\alpha_{\mathrm{IEMP}}\leqslant0.6\alpha_{\mathrm{EMP}}$). The amplitude of the IEMP is smaller because the capacitive coupling to the electrodes is less effective since the IEMP is not located above the measuring electrodes. An intrinsic lower oscillator strength can also not be ruled out.

The IEMP and EMP's are investigated in more detail as a function of temperature in sweeps from 320 to 420 kHz (Fig. 3). In the temperature range from 560 mK down to 200 mK the EMP's are nearly independent of temperature, in agreement with Ref. 24. It should be noted that the outer part of the electron sheet where the EMP is located is in the fluid phase in the whole temperature range of Fig. 3. The IEMP does not change much as the temperature goes down from

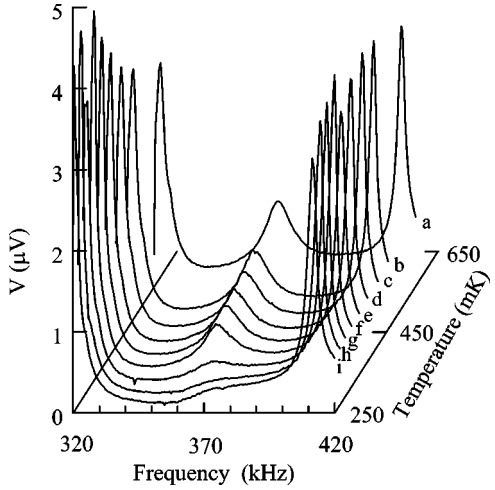

FIG. 3. Frequency spectra for the same density profile as in Fig. 2 from 320 to 420 kHz as a function of temperature: $a-i$, 563, 459, 417, 381, 349, 321, 296, 273, and 250 mK, respectively.

560 to 350 mK, but then abruptly decreases in amplitude and increases in linewidth. For the density profile used here with $n_1=2.3\times10^{12}$ m^{-2} and $n_2=0.58\times10^{12}$ m^{-2} the melting transition occurs gradually from 345 mK for the inner part to 173 mK for the outer ring. These values were calculated with the plasma parameter Γ:

$$\Gamma=\frac{e^2\sqrt{n}}{2\sqrt{\pi}(\varepsilon_r+1)\varepsilon_0 kT}, \tag{2}$$

set equal to 127.[7] So the linewidth broadening in the IEMP appears to be near the melting temperature for the inner (high-density) part of the electron sheet. It should also be noted that there is no change observable in the resonance position, from which it can be concluded that the average Hall conductivity σ_{xy} does not change upon crystallization.

B. Different electron densities

For a better analysis of the data, a way was devised to quantify the linewidth: A curve fit was made with Lorentzian curves both for the EMP's and the IEMP. From this curve fit the linewidth of the IEMP was determined. Figure 4 shows the normalized linewidths for three different inner electron densities n_1, with the same outer electron density. This should make clear whether there really is a correlation between the increase in linewidth from the IEMP and crystallization of the high-density region of the electron sheet. The melting temperatures corresponding to n_1 are indicated by the arrows. On cooling down the linewidths start to increase at the melting temperature. The data in Fig. 3 suggest that on further cooling the linewidth *gradually* increases, which could correspond to the gradual crystallization of the boundary. The rapidly increasing broadening does not allow to observe the IEMP down to the temperature where the low density region crystallizes (173 mK for the data in Fig. 3).

In the general theory,[22] the damping of the IEMP is determined by the average σ_{xx} in the boundary region. From magnetoconductivity measurements[16,17] it is known that for not too high magnetic fields σ_{xx} increases abruptly with a factor of 3 at crystallization. In the liquid phase, the temperature dependence of σ_{xx} is comparatively weak and smooth, and can be neglected in the present context. Therefore, the increase in linewidth that is observed in Fig. 4 is consistent with the expected change in σ_{xx} at the crystallized side of the boundary.

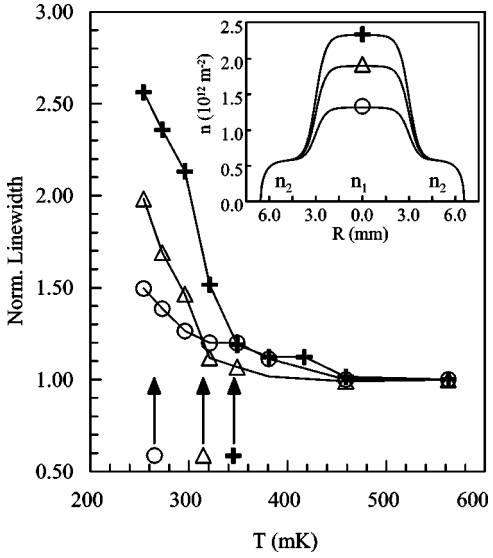

FIG. 4. Normalized linewidth for three different inner electron densities n_1: +, 2.3×10^{12}; △, 1.9×10^{12}; and ○, 1.3×10^{12} m^{-2}. $n_2=0.58\times10^{12}$ m^{-2}. Inset: Density profiles for the three measurements.

An EMP can be considered at first view as an IEMP with $n=0$ (and thus $\sigma_{xx}=0$) at one side. But then one would also expect a change in linewidth at crystallization for the EMP, which is in contrast with what is observed in earlier measurements.[18,23,24] The different behavior of EMP's and IEMP's with respect to crystallization apparently is related to the differences in density profiles at the interedge or edge (see inset of Fig. 4). In general the IEMP is much less localized than the EMP, which makes it more likely that the IEMP is sensitive to crystallization of the high-density region whereas the EMP is not.

C. Different density profiles

To verify that it is really the absolute density that is responsible for the increase in linewidth, different density profiles are studied. In Fig. 5 measurements for three different density profiles are shown, all with the same resonance frequency for the IEMP of approximately 150 kHz (i.e., $\alpha|n_1-n_2|$ is equal for all measurements). The resonance frequency of the EMP is determined by n_2, which is approximately the same for (a) and (b) and a factor of 2.25 higher for (c). Therefore the EMP is not visible in (c). For each profile two measurements are shown. One at a temperature of 563 mK, far above the melting temperature for a density of 1.3×10^{12} m^{-2} ($T_c=260$ mK). The other measurement (at either 250 or 205 mK) is done below this melting temperature. In the ring structure with $n_1=0$, no temperature effect is observed, consistent with a liquid phase at both temperatures. In curves (b) and (c) when the high-density region is crystallized at the lowest temperature, a linewidth broadening indeed occurs.

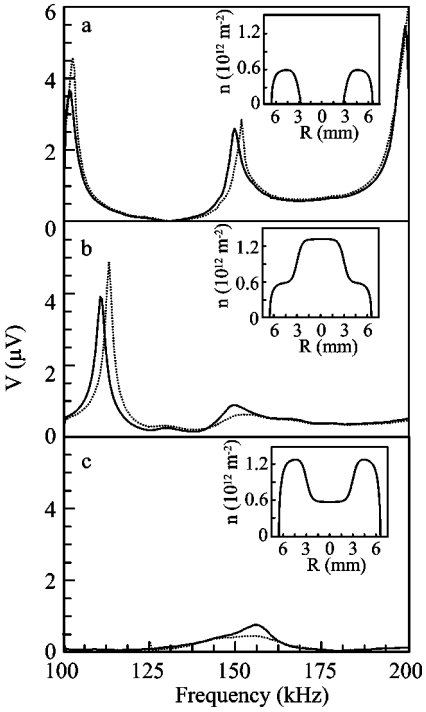

FIG. 5. IEMP resonance for three different density profiles at 563 mK (solid line) and 250 mK (a) and (b) and 200 mK (c) (dotted line). Insets: density profiles.

The data in Figs. 5(b) and 5(c) show an interesting asymmetry in line shape in the liquid phase, which clearly correlates with the density profile. Overall the linewidth for the ring structure is smaller than for the other profiles. This was also observed in Ref. 23 and is probably related to the higher α for this profile.

D. Nonlinearities

Experiments[16,17,27] have shown that there is a remarkable difference between the fluid and the solid phase with respect to the dependence on the drive voltage of the magnetoconductivity. In the fluid phase the $\sigma_{xx}(B)$ is independent of the drive voltage (except for a small deviation at very high drive voltages, which may be related to hot-electron effects), but in the solid phase a linear increase of the magnetoconductivity as a function of the drive was observed up to a certain drive voltage. At a threshold voltage σ_{xx} decreases suddenly. Since according to the theory of Ref. 22 the linewidth of the IEMP is directly proportional to the average magnetoconductivity, it is of interest to study the drive voltage dependence. Measurements have been done as a function of the drive voltage again at the two temperatures that were used in the last section: 563 mK where all electrons are in the fluid phase and 205 mK where the high-density part of the electrons (here the outer ring) are expected to have crystallized. The inner electron density n_1 was equal to 0.58×10^{12} m^{-2}, $n_2=1.3\times10^{12}$ m^{-2}. In Fig. 6 IEMP resonances are shown for four different drive voltages: 10, 15, 20, and 25 mV. To exclude the trivial linear drive voltage dependence the amplitudes are divided by the ratio of the used drive voltage and 10 mV. For the high temperature the resonances all fall on top of each other, indicating that the drive voltages are in the linear regime, so the conductivity is indeed independent of

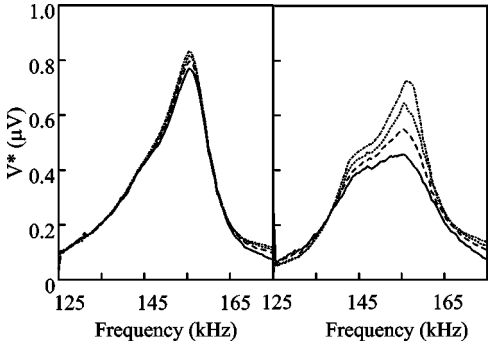

FIG. 6. Drive voltage dependence at 563 mK (left) and 200 mK (right). V^* is equal to the measured voltage divided by the ratio of the used drive voltage and 10 mV. Used drive voltages: 10 (solid line), 15 (dashed line), 20 (dotted line), and 25 mV (dashed-dotted line).

the drive voltage. This is, however, not the case for the resonances at the lower temperature. Here it can be seen that for the lowest driving voltages the resonance is broad and the amplitude is lower than in the fluid, consistent with Fig. 3. Increasing the excitation voltage leads to a more than linear increase in the amplitude, and a decrease in linewidth. For the highest drive voltage the amplitude approaches the one in the fluid phase. The drive voltage dependence, therefore, is consistent with electric-field-induced melting. It is not consistent with the observed increase of σ_{xx} with drive voltage in Ref. 16 which would lead to an increase in linewidth. No sudden changes in linewidth analogous to sudden changes in σ_{xx} as in Ref. 16 are observed in the present measurements. However, the voltages that are used in our measurements are lower than the threshold voltage in Ref. 16.

IV. CONCLUSIONS

It is clearly shown that the linewidth of IEMP's increases when the temperature is lowered below the melting temperature of the high-density region. All data are consistent with the disappearance of IEMP's when electrons in the region where the IEMP is located are crystallized. Such a condition cannot be reached with an outer edge of a sample, and explains the observed weak dependence of EMP's upon crystallization. Qualitatively, the temperature dependence is consistent with the known behavior of σ_{xx} upon crystallization. The drive voltage dependence suggests, however, that this might be a coincidence and that the melting explicitly controls the IEMP behavior. Thus we conclude that interedge magnetoplasmons could be exploited as a tool to investigate the crystallization process of a two-dimensional electron system, in particular, for inhomogeneous systems, but are not a probe for the crystal itself, or for the magnetoconductivity of the crystal.

ACKNOWLEDGMENTS

The EU is acknowledged for support from the HCM program (ERBCHBICT930490 and ERBCHRXCT930374). We would like to thank A.T.A.M. de Waele for his interest in this work.

*Present address: Technology Group, Philips Microelectronic Modules, Kreuzweg 60, D-47809 Krefeld, Germany.
[1] R. S. Crandall and R. Williams, Phys. Lett. **34A**, 404 (1971).
[2] E. Wigner, Phys. Rev. **46**, 1002 (1934).
[3] J. N. Tan, J. J. Bollinger, B. Jelenkovic, and D. J. Wineland, Phys. Rev. Lett. **75**, 4198 (1995).
[4] J. H. Chu and Lin I, Phys. Rev. Lett. **72**, 4009 (1994); H. Thomas, G. E. Morfill, V. Demmel, J. Goree, B. Feuerbacher, and D. Möhlmann, *ibid.* **73**, 652 (1994).
[5] C. A. Murray and D. H. Van Winkle, Phys. Rev. Lett. **58**, 1200 (1987).
[6] C. J. Mellor and W. F. Vinen, Surf. Sci. **229**, 368 (1990).
[7] C. C. Grimes and G. Adams, Phys. Rev. Lett. **42**, 795 (1979).
[8] For a general review see, e.g., *Two-Dimensional Electron Systems on Helium and Other Cryogenic Substrates*, edited by E. Y. Andrei (Kluwer, Dordrecht, 1997).
[9] F. M. Peeters and P. M. Platzman, Phys. Rev. Lett. **50**, 2021 (1983).
[10] G. Mistura, T. Günzler, S. Neser, and P. Leiderer, Phys. Rev. B **56**, 8360 (1997).
[11] D. Marty, J. Poitrenaud, and F. I. B. Williams, J. Phys. (France) Lett. **41**, L311 (1980); D. Marty and J. Poitrenaud, J. Phys. (France) **45**, 1243 (1984).
[12] G. Deville, A. Valdes, E. Y. Andrei, and F. I. B. Williams, Phys. Rev. Lett. **53**, 588 (1984).
[13] F. Gallet, G. Deville, A. Valdes, and F. I. B. Williams, Phys. Rev. Lett. **49**, 212 (1982).
[14] M. A. Stan and A. J. Dahm, Phys. Rev. B **40**, 8995 (1989).
[15] A. O. Stone, M. J. Lea, P. Fozooni, and J. Frost, J. Phys.: Condens. Matter **2**, 485 (1990).
[16] A. Kristensen, K. Djerfi, P. Fozooni, M. J. Lea, P. J. Richardson, A. Santrich-Badal, A. Blackburn, and R. W. van der Heijden, Phys. Rev. Lett. **77**, 1350 (1996).
[17] K. Shirahama and K. Kono, Phys. Rev. Lett. **74**, 781 (1995); K. Shirahama and K. Kono, J. Low Temp. Phys. **104**, 237 (1996).
[18] D. C. Glattli, E. Y. Andrei, G. Deville, J. Poitrenaud, and F. I. B. Williams, Phys. Rev. Lett. **54**, 1710 (1985).
[19] D. B. Mast, A. J. Dahm, and A. L. Fetter, Phys. Rev. Lett. **54**, 1706 (1985).
[20] P. J. M. Peters, M. J. Lea, A. M. L. Janssen, A. O. Stone, W. P. N. M. Jacobs, P. Fozooni, and R. W. van der Heijden, Phys. Rev. Lett. **67**, 2199 (1991); P. K. H. Sommerfeld, P. J. M. Peters, H. F. W. J. Vorstenbosch, R. W. van der Heijden, A. T. A. M. de Waele, and M. J. Lea, Physica B **194-196**, 1311 (1994).
[21] V. A. Volkov and S. A. Mikhailov, in *Modern Problems in Condensed Matter Sciences*, edited by V. M. Agranovich and A. A. Maradudin (North-Holland, Amsterdam, 1991), Vol. 27.2, p. 855.
[22] S. A. Mikhailov and V. A. Volkov, J. Phys.: Condens. Matter **4**, 6523 (1992).
[23] P. K. H. Sommerfeld, P. P. Steijaert, P. J. M. Peters, and R. W. van der Heijden, Phys. Rev. Lett. **74**, 2559 (1995).
[24] S. I. Ito, K. Shirahama, and K. Kono, J. Phys. Soc. Jpn. **66**, 533 (1996); Yu. P. Monarkha, S. I. Ito, K. Shirahama, and K. Kono, Phys. Rev. Lett. **78**, 2445 (1997).
[25] D. C. Glattli, E. Y. Andrei, G. Deville, and F. I. B. Williams, Surf. Sci. **170**, 70 (1986).
[26] A. M. C. Valkering, P. K. H. Sommerfeld, R. W. van der Heijden, and A. T. A. M. de Waele, Czech. J. Phys. **46**, 323 (1996).
[27] R. Giannetta and L. Wilen, Solid State Commun. **78**, 199 (1991).